Available online at www.sciencedirect.com
ScienceDirect
Journal of Sound and Vibration 305 (2007) 432–456
JOURNAL OF SOUND AND VIBRATION
www.elsevier.com/locate/jsvi

A simplified model to explore the root cause of stick–slip vibrations in drilling systems with drag bits

Thomas Richard[a], Christophe Germay[b], Emmanuel Detournay[c,*]

[a]CSIRO Petroleum, Technology Park Kensington, 6151 WA, Australia
[b]Institut d'Electricité Montéfiore, University of Liège, B-4000 Liège, Belgium
[c]Department of Civil Engineering, University of Minnesota, Minneapolis, MN 55455, USA

Received 5 October 2005; received in revised form 2 April 2007; accepted 4 April 2007
Available online 13 June 2007

Abstract

In this paper a study of the self-excited stick–slip oscillations of a rotary drilling system with a drag bit, using a discrete model that takes into consideration the axial and torsional vibration modes of the system, is described. Coupling between these two vibration modes takes place through a bit–rock interaction law, which accounts for both the frictional contact and the cutting processes. The cutting process introduces a delay in the equations of motion that is responsible for the existence of self-excited vibrations, which can degenerate into stick–slip oscillations and/or bit bouncing under certain conditions. From analysis of this new model it is concluded that the experimentally observed decrease of the reacting torque with the angular velocity is actually an expression of the system response, rather than an intrinsic rate dependence of the interface laws between the rock and the drill bit, as is commonly assumed.

1. Introduction

Rotary drilling systems used to drill deep boreholes for hydrocarbon exploration and production often experience severe torsional vibrations, called stick–slip, characterized by (i) sticking phases where the bit stops, and (ii) slipping phases where the angular velocity of the tool Ω increases up to two times the imposed angular velocity. This problem is particularly acute with drag bits, which consist of fixed blades or cutters mounted on the surface of a bit body.

The stick–slip phenomenon has been the subject of intensive research in various fields of mechanics [1,2], ranging from the triggering of earthquakes [3–5] to the squealing of brakes [6]. It is usually assumed that the cause of stick–slip lies within the constitutive properties of the frictional interface, and in particular through the dependence of the coefficient of friction μ on the relative velocity $[v]$ between the two contacting surfaces. In fact, stick–slip oscillations are classically modeled on the basis of a friction coefficient decreasing with $[v]$, as observed in some experiments [7–9]. Indeed, a sufficient condition to trigger instability of steady sliding is simply $\partial\mu/\partial[v]<0$ in the neighborhood of the trivial solution [10]. Due to this velocity-weakening property, the

*Corresponding author. Tel.: +1 612 625 3043; fax: +1 612 626 7750.
E-mail address: detou001@umn.edu (E. Detournay).

0022-460X/$ - see front matter © 2007 Elsevier Ltd. All rights reserved.
doi:10.1016/j.jsv.2007.04.015

frictional force acts as a negative damping and is responsible for the growth of instabilities leading eventually to stick–slip oscillations.

Field and laboratory drilling experiments often also exhibit a monotonic decrease of the mean torque $\langle T \rangle$ (averaged over several bit revolutions) with the imposed angular velocity Ω_o, under constant weight-on-bit [11,12]. These experimental observations have served as a basis for analyzing stick–slip torsional oscillations of drag bits using a torsional model of the drillstring with a velocity-weakening bit–rock interface [13–16]. However, the central question that has to be addressed in modeling this class of problems is whether the observed decrease of the torque with the angular velocity is an intrinsic property of the interface between the bit and the rock, or rather an apparent property that reflects not only the interface but also the drilling system.

Outside the particular problem of drilling, there are examples of stick–slip phenomena that can also be explained by a coupling at the frictional interface between two modes of vibrations. For example, elastic contact normal to the frictional interface has been invoked to model the stick–slip phenomenon [17–19], based on experiments showing that sliding events were accompanied by motion in the normal direction [20]. Moreover, a decrease of the apparent friction coefficient is predicted with increasing relative velocity during stick–slip oscillations [17]. The stability of surface waves along an interface characterized by a constant friction coefficient has also been studied [21–24]. The steady solutions are shown to be unstable, with the perturbed motion eventually reaching a periodic state with regions of stick and regions of slip. The coupling between the normal and the tangential displacement at the interface is the primary cause of stick–slip oscillations, with the presence of stick–slip waves causing an apparent decrease of the coefficient of friction [24].

The motivation to challenge the classical approach in the context of drilling vibrations involving drag bits stems from several observations. First, a comprehensive analysis of published laboratory data (see Appendix A) within the framework of a bit–rock interface model [25] does not support the existence of a rate-dependent bit–rock interface law. Furthermore, rate effects taking place over a time scale much smaller than the period of stick–slip (which varies typically from 1 to 3 s or equivalently from 0.5 to 10 revolutions) would need to be assumed, in order to model stick–slip oscillations provoked by a velocity-weakening law. However, there is no evidence that this effect is a constitutive property of the bit–rock interface and furthermore that it exists at time scales much smaller than the time for one revolution of the bit.

Based on the analysis of chattering in metal machining [26–29], the history dependent nature of the bit–rock interface has been proposed as possible cause of axial self-excited vibrations [30–35]. In this approach, the axial vibrations are sustained by the regenerative effect associated with drilling; namely the thickness of rock removed by a cutter is affected by the path of the cutter ahead. Self-excited torsional vibrations via coupling with the axial mode through the cutting process at the bit–rock interface have also been considered [33], but with the analysis limited to the effect of the torsional mode on the stability of the axial mode.

In this paper, we propose an alternative approach based on a discrete model of the drilling system, and on a rate-independent description of the bit–rock interaction. This model takes into consideration the axial and torsional vibration modes and their coupling through bit–rock interaction laws, which account for both frictional contact and cutting processes at the bit–rock interface. We show that this model experiences self-excited vibrations, which can degenerate into stick–slip oscillations or bit bouncing under certain conditions. Furthermore, from our analysis we observe that the decrease of the torque with the bit angular velocity is the consequence of a reduced description of the physical system, rather than the cause of the self-excitations.

2. Mathematical formulation

In this section, we describe a simplified model to study the self-excited axial-torsional vibrations of a drilling system. First, we discuss a reduced two degrees of freedom system and the justification for this particular discrete model. Then we focus on the characterization of a rate-independent bit–rock interface law, starting with the interaction between a single cutter and a rock. The interaction law accounts both for cutting of the rock and for frictional contact on the cutter wearflat. The cutting forces are formulated in terms of the depth of cut, a variable which brings into the equations the position of the bit at a previous a priori unknown time. Combining the equations governing the discrete system with the interface law leads to the formulation of a novel state-dependent delay dynamical system, with discontinuous boundary conditions that reflects loss of contact at the wearflat/rock interface caused by small amplitude axial vibrations of the bit.

2.1. Model of the drilling system

A rotary drilling structure consists essentially of a rig, a drill string, and a bit. The principal components of the drill string are the bottom hole assembly (BHA) composed mainly of heavy steel tubes to provide a large downward force on the bit, and a set of drillpipes made of thinner tubes. For the idealized drilling system under consideration, we assume: (i) that the boundary conditions applied by the rig to the top of the drillstring correspond to a constant upward force H_o and a constant angular velocity Ω_o, (ii) that the borehole is vertical, and (iii) that there are no lateral motions of the bit. The nature of the boundary conditions at the bit–rock interface is a critical aspect of the model and is discussed in details below.

The bit motion as well as the forces acting on the bit can in principle be calculated knowing the prescribed surface boundary conditions, the mechanical properties of the drill string and the bit–rock interaction law. For this analysis, we consider a discrete model of the drilling system characterized by only two degrees of freedom, U and Φ, corresponding to the vertical and angular position of the bit, respectively, and by three mechanical elements, namely a point mass M, a moment of inertia I and a spring of torsional stiffness C, see Fig. 1. The mass M and the moment of inertia I are taken to represent the BHA, while the spring C is assumed to stand for the torsional stiffness of the drillpipe. However, I is corrected to account for the inertia of the drillpipes, in order to improve the estimate of the period of free torsional vibrations [36]. Expressions for M, I, and C are readily obtained by assuming that both the drillpipes and the BHA correspond to continuous shafts with constant cross-section and density ρ

$$M = \rho\pi(r_{bo}^2 - r_{bi}^2)L_b, \quad I = \rho J_b L_b + \frac{1}{3}\rho J_p L_p, \quad C = \frac{GJ_p}{L_p}, \tag{1}$$

with

$$J_p = \frac{\pi}{2}(r_{po}^4 - r_{pi}^4), \quad J_b = \frac{\pi}{2}(r_{bo}^4 - r_{bi}^4)$$

and with r_{pi} (r_{bi}), r_{po} (r_{bo}), L_p (L_b), J_p (J_b) denoting, respectively, the inner radius, outer radius, length, and polar moment of inertia of the drillpipe (bottom hole assembly).

Reduction of the continuous system, consisting of drillpipes and the bottom hole assembly, to a two degrees of freedom system is motivated by the need to define a reasonable yet tractable model to assess the consequence of the nature of the boundary conditions at the bit–rock interface. Nonetheless, these simplifications are in part substantiated by field measurements indicating that the torsional oscillations of the

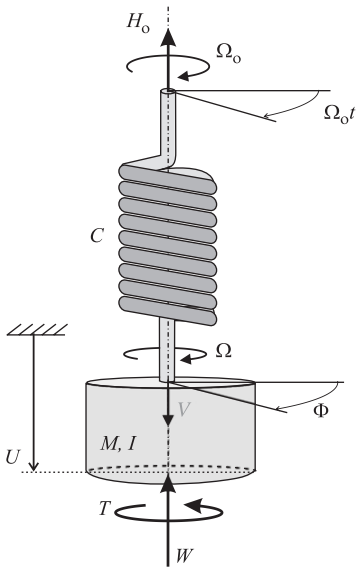

Fig. 1. Sketch of a simplified model of the drilling system.

drill bit are dominated by the first mode of vibrations of the drilling system. In fact, these field observations have often justified the reduction of the drilling system to a torsional pendulum [37]. We have also chosen to neglect any damping of the system as most of the energy dissipation in drilling systems is taking place at the bit–rock interface; this dissipation is accounted for by the bit–rock interaction laws discussed below.

The asymmetry in the axial and torsional description of the reduced system stems from the different nature of the two boundary conditions at the rig: "fixed" in rotation (i.e., imposed angular position $\Omega_o t$), and "free" in translation (i.e., imposed constant axial force H_o). These boundary conditions at the top of the drill string imply that the axial stiffness of the pipes can be disregarded in this particular discrete model. Despite neglecting the axial stiffness, non-trivial axial motions of the bit arise from the coupling between the two vibration modes through the bit–rock interaction.

Given the constant angular velocity Ω_o and constant upward tension H_o imposed to the upper end of the torsional spring, we seek to determine the unknown bit response $\mathscr{R}(t) = \{W(t), V(t), T(t), \Omega(t)\}$. This response, which is generally a function of time t, consists of two sets of conjugated dynamical and kinematical quantities: the weight-on-bit W and the vertical bit velocity $V = \mathrm{d}U/\mathrm{d}t$ (also called rate of penetration) on the one hand, and the torque-on-bit T and the angular bit velocity $\Omega = \mathrm{d}\Phi/\mathrm{d}t$ on the other hand. (Refer to Fig. 1 for the sign convention adopted for these quantities.)

2.2. Bit–rock interface

As an introduction to the formulation of the bit–rock interface laws, we first consider the forces acting on a single cutter, which is steadily removing rock over a constant depth, as illustrated in Fig. 2. The action of such a tool generally consists of two independent processes [25]: (i) a pure cutting process taking place ahead of the cutting face, and (ii) a frictional contact process mobilized along the interface between the wearflat and the rock. The force $\mathbf{F}$ on the cutter results therefore from the superposition of two forces $\mathbf{F}_c$ and $\mathbf{F}_f$, acting on the cutting face and on the wearflat, respectively. Provided that these forces are averaged over a distance equal to at least a few times the depth of cut, $\mathbf{F}_c$ and $\mathbf{F}_f$ can be treated as being steady [25,38], and thus only four parameters are needed to characterize their magnitude and inclination. The components of these two forces in a direction parallel (subscript s) and perpendicular (subscript n) to the cutter motion, i.e., $\mathbf{F}_c = (F_{cs}, F_{cn})^{\mathrm{T}}$, $\mathbf{F}_f = (F_{fs}, F_{fn})^{\mathrm{T}}$, can be expressed as (see Fig. 2)

$$F_{cs} = \varepsilon w d, \quad F_{cn} = \zeta F_{cs}, \quad F_{fs} = \mu F_{fn}, \quad F_{fn} = \sigma w \ell, \tag{2}$$

where ε is the intrinsic specific energy, a parameter related to the rock strength under certain conditions [39], ζ is a number characterizing the orientation of the cutting force $\mathbf{F}_c$, μ is a coefficient of friction that is well correlated to the internal friction angle of the rock [40–42] , and σ is the maximum contact pressure at the wearflat/rock interface, a parameter which is of the same order as ε [40,41]. The expressions for F_{cs} and F_{fn} in Eq. (2) are specific for a constant cutter width w, but they hold more generally provided that wd is replaced by the cross-sectional area of the groove traced by the cutter and $w\ell$ by the wearflat area, with d denoting the depth of cut and ℓ the length of the wearflat.

The presence of a contact surface between the rock and the cutter, subparallel to the average direction of cutter motion, has significant implications in regard to the variation of the force acting on the cutter, caused by a perturbation in the direction of cutter velocity $\mathbf{v}$. We consider a perturbation in the form of a velocity

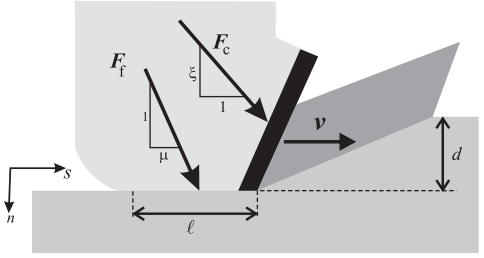

Fig. 2. Sketch of the repartition of the forces acting on a single cutter.

component v_n (small compared to v_s) which is superimposed on the initial velocity v_s. If $v_n<0$ (leading to a decreasing depth of cut), there is a momentary loss of contact at the wearflat interface that is associated with a discontinuous force response as $\mathbf{F}$ becomes suddenly equal to $\mathbf{F}_c$. If $v_n>0$, the force on the cutter will increase monotonically in view of the dependence of the magnitude of the cutting force on the depth of cut (with the force $\mathbf{F}_f$ remaining virtually unchanged). We will also interpret the expression for F_{fn} in Eq. (2) to imply that the cutter is only in frictional contact with the rock (i.e. $d=0$) if $F_n<\sigma w\ell$. In reality, some cutting is taking place when $F_n<\sigma w\ell$ but how much rock is removed depends on how the wearflat is in conforming contact with the rock.

These concepts can be extended to model the generalized forces acting on a drill bit by integrating the effects of all the individual cutters [25]. The torque T and weight-on-bit W can also be decomposed into a contribution associated to the forces transmitted by the cutting face of each cutter (denoted by the subscript c) and another corresponding to the forces acting on the cutter wearflats (denoted by the subscript f)

$$T = T_c + T_f, \quad W = W_c + W_f. \tag{3}$$

The cutting components of the torque T_c and weight W_c can be written as

$$T_c = \tfrac{1}{2}\varepsilon a^2 d, \quad W_c = \zeta \varepsilon a d, \tag{4}$$

while the torque T_f and weight-on-bit W_f are related according to

$$2T_f = \mu a \gamma W_f. \tag{5}$$

In the above equations, a denotes the bit radius and γ is a bit geometry number (greater than 1) that characterizes the orientation and spatial distribution of the frictional contact surfaces associated with the cutters.

The expressions in Eq. (4) for T_c and W_c, which echo the expressions in Eq. (2) for the forces F_{cs} and F_{cn} on a single cutter, are assumed to be valid at any moment as the averaging of the forces fluctuations on all the cutters of the bit has the same effect as the averaging over distance implied for a single cutter.

The instantaneous depth of cut d, which appears in Eq. (4), is most easily interpreted by restricting consideration to an idealized drag bit consisting of n identical radial blades regularly spaced by an angle equal to $2\pi/n$ (see Fig. 3). Each blade is characterized by a sub-vertical cutting surface and a chamfer of constant width ℓ_n orthogonal to the cutting face. When such a bit is drilling rock, and in the absence of any lateral motion, the depth of cut per blade d_n (i.e., the thickness of the rock ridge in front of the blade) is constant along the blade and identical for each blade. Furthermore, d_n is related to the vertical position of the bit U according to

$$d_n(t) = U(t) - U(t - t_n), \tag{6}$$

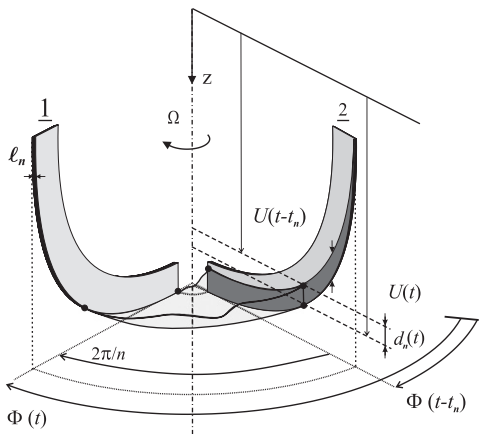

Fig. 3. Section of the bottom-hole profile located between two successive blades of a drill bit, which is characterised by n identical blades symmetrically distributed around the axis of revolution. The thickness of each blade ℓ_n corresponds to the length of wearflat per cutter.

where t_n (t) is the time required for the bit to rotate by an angle $2\pi/n$ to its current position at time t, as schematically illustrated in Fig. 3. The delay $t_n(t)$ is solution of

$$\Phi(t) - \Phi(t - t_n) = 2\pi/n. \tag{7}$$

The equivalent wearflat length for the bit is $\ell = n\ell_n$ and the combined depth of cut of the bit is simply $d = nd_n$ or

$$d = n[U(t) - U(t - t_n)]. \tag{8}$$

The depth of cut d appearing in Eq. (4) also represents the depth of cut per revolution of the bit, i.e., $d = 2\pi V/\Omega$, under steady conditions or when it is averaged over several revolutions.

The additional relationship needed to resolve the depth of cut d corresponding to a prescribed W depends on the direction of the instantaneous axial bit velocity, which impacts on W_f as discussed below. Irrespective of the magnitude of W_f and T_f, however, a constraint on the bit response can be deduced by combining Eqs. (3)–(5) to yield

$$\frac{2T}{a^2} = (1 - \beta)\varepsilon d + \mu\gamma\frac{W}{a}, \tag{9}$$

with

$$\beta = \mu\gamma\zeta. \tag{10}$$

The linear constraint given in Eq. (9) applies as long as the bit is drilling.

The interaction between the bit and the rock can be classified into the following four modes:

- *Cutting* ($\Omega > 0$, $d > 0$). Consider first the "normal case" when $V > 0$. The cutting and frictional components of W and T are explicitly given by Eq. (4) and

$$W_f = a\ell\sigma, \quad T_f = \frac{a^2}{2}\gamma\mu\ell\sigma, \tag{11}$$

  where the average contact pressure σ is assumed to be constant when $V > 0$ and $\Omega > 0$ and the bit is cutting ($d > 0$). Thus drilling occurs in the normal case, only if $W > W_f$ and $T > T_f$. Consider next the case $V < 0$ and $\Omega > 0$ when the bit is moving upwards. We assume a complete loss of contact between the wearflat and the rock, so that the frictional components W_f and T_f vanish. Hence $W = W_c$ and $T = T_c$, as long as $d > 0$. When $V = 0$, $W_f = W_o - W_c$.
- *Sticking* ($\Omega = 0$, $d > 0$). During the stick phase the bit remains immobile. In this case, d represents the "step" in front of the blades that dictates the minimum forces (W, T) to be applied in order to exit the stick mode. During this phase, $V = 0$, $U = U(t_k)$ and $\Phi = \Phi(t_k)$ with t_k denoting the time at which the bit sticks. We assume complete contact between the wearflat (or chamfer) and the rock during the sticking phase.
- *Sliding* ($\Omega > 0, d = 0$). In sliding mode, the rate of penetration V and the cutting components of the forces (T_c, W_c) vanish.
- *Off-bottom* ($\Omega > 0, d < 0$). The bit is not in contact with the hole bottom and thus $T = W = 0$. Such a complete loss of contact between the bit and the rock takes place during bit bouncing.

2.3. Governing equations

The non-trivial bit response $\mathscr{R}(t) = \{W(t), V(t), T(t), \Omega(t)\}$ can, in principle, be determined from the surface conditions and the bit–rock interface laws, together with the following torsional and axial equations of motion:

$$I\frac{\mathrm{d}^2\Phi}{\mathrm{d}t^2} + C(\Phi - \Phi_o) = T_o - T({}^t_0\Phi, {}^t_0U),$$
$$M\frac{\mathrm{d}^2U}{\mathrm{d}t^2} = W_o - W({}^t_0\Phi, {}^t_0U), \tag{12}$$

where Φ_o, T_o, and W_o are the stationary quantities associated with the trivial solution, see Eqs. (15) and (18). In view of the nature of the interaction laws discussed above, both T and W are actually functions of the history of Φ (denoted by ${}^{t}_{0}\Phi$) and the history of U (denoted by ${}^{t}_{0}U$). Indeed the cutting components of T and W are proportional to the depth of cut d, a state variable that is defined by comparing the current bit position $U(t)$ to a previous position $U(t-t_n)$ in accordance with Eq. (8), with the delay t_n solution of Eq. (7). The system of equations in Eq. (12) represent a retarded dynamical system [43]. Furthermore, this system is characterized by a state-dependent delay [44], unlike similar systems that arise from the modeling of various metal machining processes for which the delay can be assumed to be constant [27,29].

An additional complexity of the model arises from the discontinuous nature of the boundary conditions during stick–slip. For the sake of simplicity, we assume that the frictional component of the torque is sufficient to hinder any backward rotation of the bit. Therefore, the condition for the bit to stick at time t_k is

$$\frac{\mathrm{d}\Phi}{\mathrm{d}t} = 0 \quad \text{at } t = t_k. \tag{13}$$

During the stick phase, rotation of the drill pipes continues at the surface, the torque applied by the drill pipes upon the bottom hole assembly, $T = C(\Phi - \Omega_o t)$, builds up until its magnitude is sufficient to overcome the torque $(T_c + T_f)$ necessary to cut the rock. Thus the bit slips at time t_p, given by the solution of

$$C(\Omega_o t_p - \Phi_k) = \frac{a^2}{2}(\varepsilon d_k + \mu\gamma\ell\sigma), \tag{14}$$

where $\Phi_k = \Phi(t_k)$ and $d_k = d(t_k)$.

2.4. Steady-state solution

There is a steady-state (trivial) response of the bit, $\mathscr{R}_o = \{W_o, V_o, T_o, \Omega_o\}$, which is characterized by

$$W_o = W_s - H_o, \quad \Omega = \Omega_o, \quad \Phi_o = \Omega_o t - T_o/C, \tag{15}$$

where W_s is the submerged weight of the drill string. Steady-state drilling conditions represent particular instances of the normal case ($V>0$, $\Omega>0$). The delay t_{no} is here constant and given by

$$t_{no} = \frac{2\pi}{n\Omega_o} \tag{16}$$

and thus the depth of cut is

$$d_o = \frac{2\pi V_o}{\Omega_o}. \tag{17}$$

The penetration rate V_o and torque-on-bit T_o are readily deduced from the bit–rock interaction laws given in Eqs. (3) and (4), thus

$$V_o = \frac{(W_o - W_f)\Omega_o}{2\pi a\zeta\varepsilon}, \quad T_o = T_f + \frac{a(W_o - W_f)}{2\zeta} \quad \text{if } W_o > W_f. \tag{18}$$

The bit is not drilling if $W_o \leqslant W_f$, i.e., $V_o = 0$ and $T_o = a\gamma\mu W_o/2$. Hence the steady-state solution is fully defined by the bit–rock interface and the control parameters, as it is not affected by the inertia and stiffness of the drilling system.

3. Scaling

We show now that the 13 physical parameters controlling the dynamical system can be reduced, by scaling, to 6 dimensionless quantities. The dimensionless formulation hinges on introducing a time scale that reflects the global response of the drilling structure and a length scale that embodies the interaction between the bit and the rock. The time scale is proportional to the period of the first resonant mode of torsional oscillations while the length scale is a characteristic depth of cut. These two scales echo the multiscale nature of this

problem, namely that vibrations of a structure with characteristic length of order of 10^3 m are triggered by cutting processes at the bit–rock interface that are characterized by depths of cut of order of 10^{-3} m.

3.1. Dimensionless formulation

To formulate the model in dimensionless form, we first need to introduce a time scale t_* and a characteristic length L_* which are defined by

$$t_* = \sqrt{\frac{I}{C}}, \quad L_* = \frac{2C}{\varepsilon a^2}. \tag{19}$$

While $2\pi t_*$ is the period of the resonant torsional vibration of the discrete drilling system, L_* represents the depth of cut when drilling with a perfectly sharp bit ($\ell = 0$) subjected to a torque that induces a twist of 1 radian in the drill string (typically, $t_* \sim 1$ s and $L_* \sim 1$ mm). The scaled kinematical and dynamical quantities at the bit, i.e. u, v, φ, ω, $\mathscr{W}$, $\mathscr{T}$, are then defined as

$$u = \frac{U - U_o}{L_*}, \quad v = \frac{V t_*}{L_*}, \quad \varphi = \Phi - \Phi_o, \quad \omega = \Omega t_*, \quad \mathscr{W} = \frac{W}{\zeta \varepsilon a L_*}, \quad \mathscr{T} = \frac{T}{C}, \tag{20}$$

where $U_o = V_o t$ is the vertical bit position according to the trivial response. Thus, u and φ represent perturbations of the axial and angular positions of the bit with respect to the trivial motion. We also define the dimensionless depth of cut δ:

$$\delta = \frac{d}{L_*}. \tag{21}$$

All these quantities are function of the scaled time τ:

$$\tau = \frac{t}{t_*}. \tag{22}$$

Note that $v = v_o + \dot{u}$ and $\omega = \omega_o + \dot{\varphi}$, with the dot denoting differentiation with respect to τ and v_o and ω_o representing the trivial dimensionless rate of penetration and bit angular velocity, respectively.

The scaled bit response $\mathscr{B}(\tau) = \{\mathscr{W}, v, \mathscr{T}, \omega\}$ depends on two classes of parameters: on the one hand the control parameters corresponding to the prescribed weight-on-bit and rotation speed

$$\mathscr{W}_o = \frac{W_o}{\zeta \varepsilon a L_*}, \quad \omega_o = \Omega_o t_*, \tag{23}$$

and on the other hand the model parameters, i.e., the number of blades n and the lumped parameters characterizing the bit geometry, its wear state, and the drilling structure:

$$n, \quad \beta = \mu\gamma\zeta, \quad \lambda = \frac{\sigma\ell}{\zeta\varepsilon L_*}, \quad \psi = \frac{\zeta\varepsilon a I}{MC}. \tag{24}$$

The typical range of variation of both control parameters is $[1, 10]$. The bluntness number λ and the bit–rock interaction number β are of order 1. The system number ψ is the only large number of this problem as it is of order 10^2–10^3; its largeness confirms that inertia of the bottom hole assembly cannot be neglected. Note that the dimensionless formulation has reduced the number of parameters from 13 $(M, I, C, \varepsilon, \mu, \sigma, \zeta, a, \gamma, \ell, n, W_o, \Omega_o)$ to 6 $(n, \lambda, \beta, \psi, \mathscr{W}_o, \omega_o)$.

3.2. Scaled mathematical model

The non-trivial response $\mathscr{B}(\tau)$ is governed by the conditions at the surface and at the bit–rock interface and by the momentum balance equations (Eq. (12)), which can be written in dimensionless form as

$$\ddot{u} = \psi(\mathscr{W}_o - \mathscr{W}), \quad \ddot{\varphi} + \varphi = \mathscr{T}_o - \mathscr{T}. \tag{25}$$

Recall that both $\mathscr{T}$ and $\mathscr{W}$ are functionals of the history of φ (denoted by ${}^{\tau}_{0}\varphi$) and u (denoted by ${}^{\tau}_{0}u$).

The bit–rock interaction laws are functions of the combined depth of cut δ for the bit. We choose to express δ in terms of a perturbation $\hat{\delta}$ from the depth of cut per revolution for the trivial motion, $\delta_o = 2\pi v_o/\omega_o$

$$\delta = \delta_o + \hat{\delta}. \tag{26}$$

The perturbation $\hat{\delta}$ is given by

$$\hat{\delta} = n v_o \hat{\tau}_n + n(u - \tilde{u}), \tag{27}$$

where $\tilde{u}(\tau) = u(\tau - \tau_n)$ is the delayed motion, and $\hat{\tau}_n = \tau_n - \tau_{no}$ with $\tau_n(\tau)$ the actual delay and $\tau_{no} = 2\pi/n\omega_o$ the constant delay for the trivial response. The algebraic equation governing the delay perturbation $\hat{\tau}_n(\tau)$ is deduced from Eq. (7) and the above definitions to be

$$\omega_o \hat{\tau}_n + \varphi - \tilde{\varphi} = 0, \tag{28}$$

with $\tilde{\varphi}(\tau) = \varphi(\tau - \tau_n)$.

The bit–rock interaction laws can be summarized as follows. If $\dot{\varphi} > -\omega_o$,

$$\mathscr{W} - \mathscr{W}_o = \hat{\delta} + \mathscr{W}_f - \lambda, \tag{29}$$

$$\mathscr{T} - \mathscr{T}_o = \hat{\delta} + \beta(\mathscr{W}_f - \lambda), \tag{30}$$

where

$$\mathscr{W}_f = \begin{cases} \lambda & \text{if } \dot{u} > -v_o, \\ 0 & \text{if } \dot{u} < -v_o. \end{cases} \tag{31}$$

If $\dot{u} = -v_o$ then $0 < \mathscr{W}_f < \lambda$ and $\mathscr{W}_f$ is deduced from the balance of linear momentum.

The bit stick at time τ_k when

$$\dot{\varphi} = -\omega_o \quad \text{at } \tau = \tau_k \tag{32}$$

and then slips at time τ_p given by

$$\tau_p = \tau_k + [\varphi(\tau_k) + \mathscr{T}(\tau_k) - \mathscr{T}_o]/\omega_o. \tag{33}$$

It is interesting to note that the prescribed rotation speed ω_o of the drill string enters the governing equations via the delay function $\tau_n(\tau)$, as a consequence of the nature of the bit–rock interface.

The system of equations that has to be solved for $\mathscr{B}(\tau)$ is unusual, in view of the delayed nature of the differential equations (with an a priori unknown delay) and their coupling through the variable δ, as well as the existence of two discontinuities (the loss of frictional contact and the stick phase). In the absence of vibrations, the response $\mathscr{B}(\tau)$ is simply the trivial solution $\mathscr{B}_o = \{\mathscr{W}_o, v_o, \mathscr{T}_o, \omega_o\}$, with v_o and $\mathscr{T}_o$ given by

$$v_o = \frac{\omega_o}{2\pi}(\mathscr{W}_o - \lambda), \quad \mathscr{T}_o = \mathscr{W}_o + \lambda(\beta - 1), \tag{34}$$

if cutting is taking place ($\mathscr{W}_o > \lambda$).

The numerical procedure used to solve the system of Eqs. (25)–(33) is discussed in Appendix C.

4. Self-excited vibrations

In this section, we demonstrate that the nonlinear dynamical system is prone to self-excited vibrations. First, we conduct a linear stability analysis that indicates that the trivial motion is unstable. This analysis is carried out on the assumption that ψ is large enough to permit approximating the state-dependent delay system as a constant delay system for which the stability conditions are known. Next we summarize the results of numerical simulations showing that the nonlinear system usually evolves towards a limit (or a quasi-limit) cycle. In particular, the existence of a limit cycle with stick–slip oscillations appears to be associated with $\beta < 1$.

4.1. Linear stability analysis

As a prelude to the numerical simulations, we investigate the evolution of small perturbations to the trivial solution in order to assess the self-excited nature of the system of equations. There are, however, hardly any published results regarding the stability of state-dependent delay system that could guide our analysis. Therefore, we first develop an argument based on the separation of time scales between the axial and torsional vibrations to justify the transformation of the dynamical system into a simplified constant delay system, for which the stability criterion is known. Furthermore, to avoid having to deal with discontinuities in the boundary conditions, the stability analysis is conducted on the assumption that the disturbances are small enough to ensure a permanent frictional contact between the bit and the rock ($\mathscr{W}_f = \lambda$).

The linearized equations governing the evolution of the perturbations are deduced from Eqs. (25), (29) and (30) to be

$$\ddot{u} = -n\psi\left[-\frac{v_o}{\omega_o}(\varphi - \breve{\varphi}) + u - \breve{u}\right], \tag{35}$$

$$\ddot{\varphi} + \varphi = -n\left[-\frac{v_o}{\omega_o}(\varphi - \breve{\varphi}) + u - \breve{u}\right], \tag{36}$$

where $\breve{u} = u(\tau - \tau_{no})$ and $\breve{\varphi} = \varphi(\tau - \tau_{no})$, thus corresponding to a constant delay ($\hat{\tau}_n = 0$). Analysis of the stability of the equilibrium points, where u is constant (implying $u = \breve{u}$) and $\varphi = 0$, of the above two equations hinges on the recognition that there is essentially a time separation between the axial and torsional dynamics in view of the largeness of ψ. Indeed, the axial perturbations u evolve relative to a time scale, which is $\psi^{1/2}$ smaller than the reference time scale for the torsional perturbations φ, as can be noted by eliminating ψ from Eq. (35) through the introduction of a stretched time $\tau' = \psi^{1/2}\tau$.

One consequence of this temporal disconnection is that the term $(\varphi - \breve{\varphi})$ in the axial equation, Eq. (35), can be treated as fixed. Furthermore, the torsional perturbations are virtually non-existent in the time boundary layer (in terms of τ') where the axial perturbations might possibly grow. Hence, the stability of the equilibrium point $u = \text{const.}$ can be assessed from the uncoupled equation [45]

$$\ddot{u} + n\psi u - n\psi\breve{u} = 0, \tag{37}$$

where Eq. (37) has been written in terms of the original time τ, and thus applies over $\tau = O(\psi^{-1/2})$.

The stability of the equilibrium point $u = 0$ can be assessed from general results obtained for the second-order delay differential equation [46,47]

$$\frac{\mathrm{d}^2}{\mathrm{d}\xi^2}x(\xi) + qx(\xi) + rx(\xi - 1) = 0. \tag{38}$$

The trivial solution $x = 0$ of Eq. (38) is stable provided that the parameters r and q are within regions bounded by the linear segments

$$r = 0, \quad r = (-1)^k[q - (k-1)^2\pi^2], \quad k = 1, 2, \ldots \tag{39}$$

as depicted in Fig. 4. Because $q = -r$ in the linearized delay equation governing the evolution of axial perturbations, the trivial solution $u = 0$ is in fact never asymptotically stable. However, $u = 0$ can still be stable in the Lyapunov sense (i.e., the solution neither diverges, nor converges) or unstable. The stability of the equilibrium point $u = \text{const.}$ (equivalent to $\dot{u} = 0$) is investigated in Appendix B, where it is shown that the equilibrium point $\dot{u} = 0$ is asymptotically stable when $\tau_{no} < \tau_{nc}$, marginally stable when $\tau_{no} = \tau_{nc}$ and unstable when $\tau_{no} > \tau_{nc}$, with the critical delay $\tau_{nc} = \pi/\sqrt{2n\psi}$.

If the equilibrium point $\dot{u} = 0$ is stable, the right-hand side of Eq. (35) vanishes for large τ'; with the implication that Eq. (36) simplifies at $\tau = O(1)$ as

$$\ddot{\varphi} + \varphi = 0. \tag{40}$$

This indicates that the torsional motion is stable if the axial motion is stable and thus suggests that axial instability is a precursor of the torsional instability.

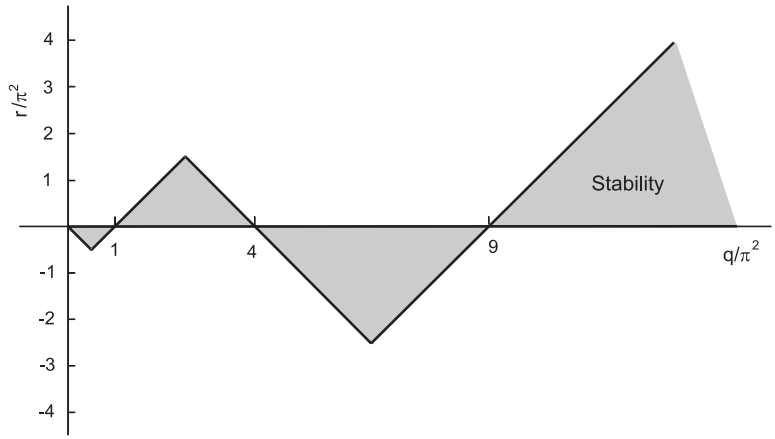

Fig. 4. Complete stability charts in the parametric space, after Refs. [47,48].

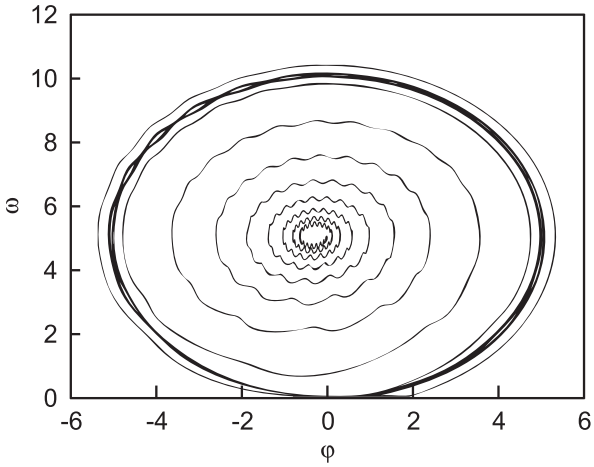

Fig. 5. Phase diagram ($n = 6$, $\psi = 50$, $\beta = 0.3$, $\omega_o = 5$, $\mathscr{W}_o = 7$, $\lambda = 5$).

4.2. Limit cycles

Extensive numerical simulations confirm that the system naturally experiences self-excited vibrations, as any perturbations to the trivial motion (even of numerical nature) cause the system to evolve towards one regime of self-excited axial and torsional vibrations. For sets of parameters representative of field values, the solution of the system evolves usually towards a periodic motion characterized either by a strict limit cycle (see Fig. 5) or by a quasi-limit cycle that evolves very slowly compared to the characteristic time of the system. Different regimes of vibrations such as stick–slip oscillations or bit bouncing are observed under different conditions.

In Fig. 6 is shown the evolution of ω, v, $\mathscr{W}$ and δ during four successive limit cycles for a typical case of stick–slip vibrations. While the angular velocity ω can be described as a quasi-monochromatic signal, with the dominant frequency slightly smaller than the natural torsional frequency of the system, the power spectrum of the axial variables is characterized by a larger spread of frequencies.

The periodic variation of the depth of cut, revealed by the polar plots of Fig. 7 showing the evolution of the depth of cut with the angular bit position, implies the formation of a repetitive geometrical bottom hole pattern. Indeed, the curves corresponding to successive limit cycles are quasi-identical, as they can virtually be superimposed after correction for a phase shift. Fig. 7 actually reflects the history-dependent nature of the system; the history of vibrations imprinted in the bottom-hole pattern encourages amplification of the self-excited vibrations.

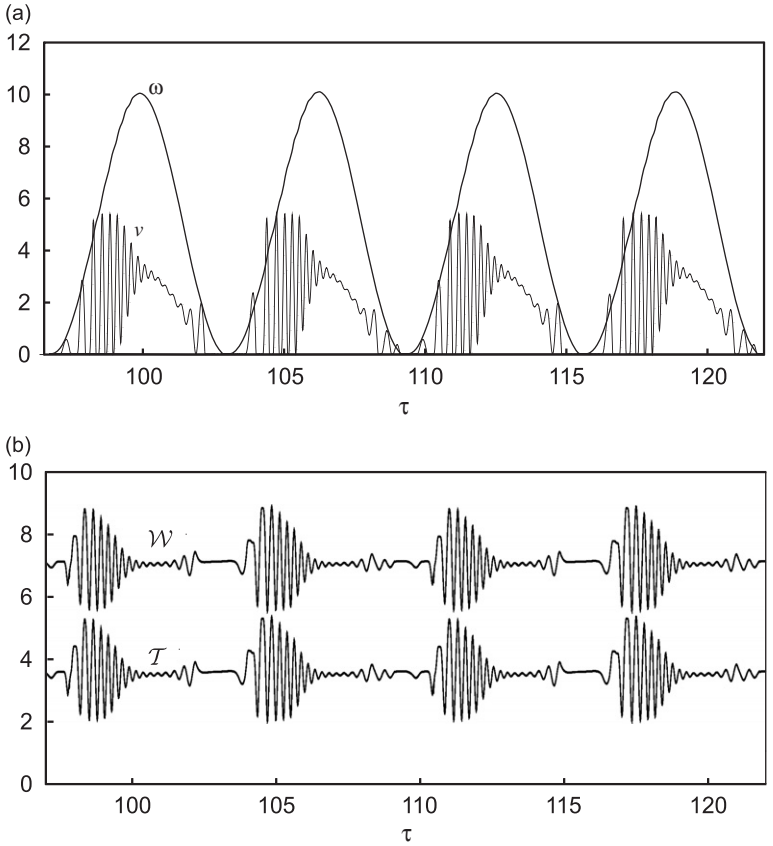

Fig. 6. Evolution with time τ of (a) ω and v, and (b) $\mathscr{T}$ and $\mathscr{W}$ ($n=6$, $\psi=50$, $\beta=0.3$, $\omega_o=5$, $\mathscr{W}_o=7$, $\lambda=5$).

4.3. Stick–slip vibrations

For typical values of the control and model parameters, β appears to be the only parameter of the model that can prohibit the occurrence of stick–slip oscillations, as all the other parameters only influence the time required to reach a steady regime of stick–slip vibrations, once the system departs the trivial solution. In fact, the threshold $\beta=1$ separates two regimes of vibrations: for $\beta<1$, the torsional oscillations grow until a limit cycle characterized by stick slip oscillations is eventually reached, while for $\beta>1$ torsional oscillations remain bounded and the system reaches a limit cycle without stick–slip. This important result is illustrated in Fig. 8, which shows the evolution of the magnitude of the torsional vibrations for $\beta=0.3$ and 1.3, following a perturbation at $t=0$. The numerical simulations remain consistent, however, with the linear stability analysis, which indicates that the system experiences self-excited vibrations irrespective of the value of β.

The critical role played by β on the existence of stick–slip vibrations can be explained by considering the time scale separation of the axial and torsional dynamics. Since the axial dynamics evolves approximately $\sqrt{\psi}$ (typically $O(10)$) faster than the torsional dynamics, only the slow variations of the fast axial variables affects the angular motion. Thus, provided that ψ is large enough, the balance of angular momentum can be simplified as

$$\ddot{\varphi}+\varphi=(\beta-1)\langle\lambda-\mathscr{W}_f\rangle_a+\frac{1}{\psi}\langle\ddot{u}\rangle_a, \tag{41}$$

with $\langle\rangle_a$ denoting an average over one *axial* limit cycle.

Moreover, the "fast" axial dynamics can be decoupled from the torsional dynamics by treating the delay as a fixed parameter over one (fast) axial limit cycle [48]. In fact, it can be shown that $\langle\ddot{u}\rangle_a=0$ for a fixed delay and that $\langle\lambda-\mathscr{W}_f\rangle_a$ increases with τ_n considered as fixed during one axial periodic orbit [49]. In the slow

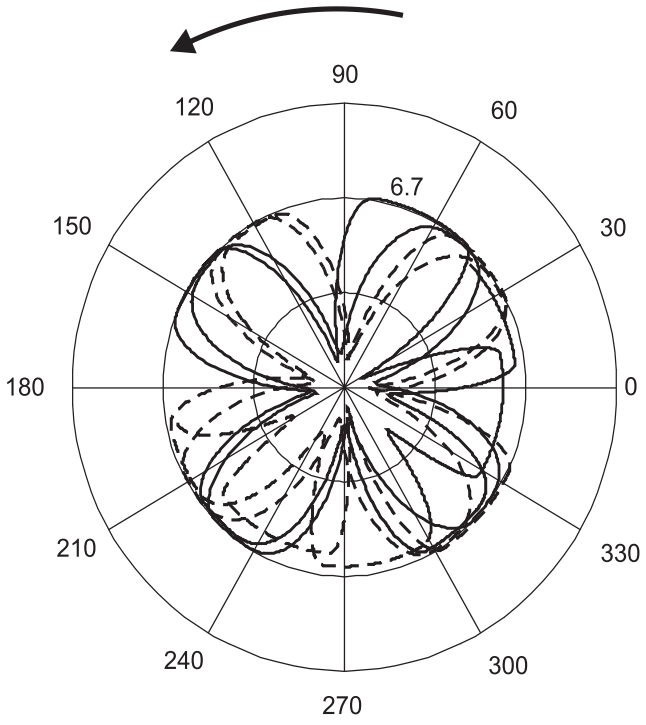

Fig. 7. Pattern of depth of cut with angular position for two successive limit cycles ($n = 6$, $\psi = 63$, $\beta = 0.28$, $\omega_o = 4$, $\mathscr{W}_o = 8$, $\lambda = 0.76$).

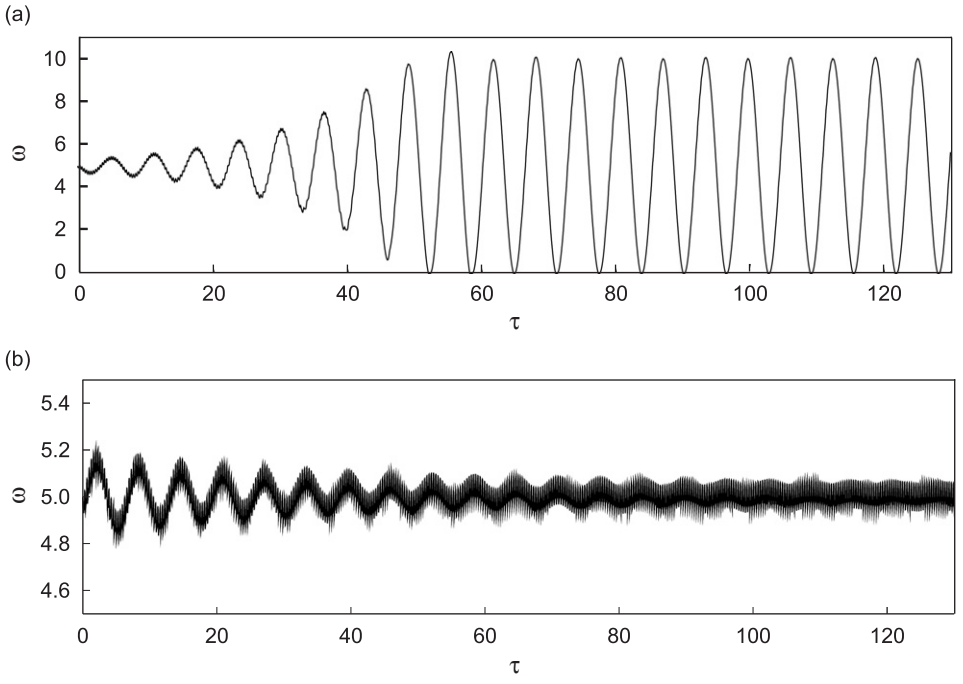

Fig. 8. Different types of evolution of the torsional vibrations for (a) $\beta = 0.3$ and (b) $\beta = 1.3$ ($n = 6$, $\psi = 50$, $\mathscr{W}_o = 7$, $\lambda = 5$, $\omega_o = 5$).

dynamics, τ_n is in a first approximation inversely proportional to ω. Hence, the quantity $\langle \lambda - \mathscr{W}_f \rangle_a$ decreases with respect to the angular bit velocity ω. Depending on the sign of $(\beta - 1)$, this term will act as positive or as negative damping. If $\beta > 1$, the term $(\beta - 1)\langle \lambda - \mathscr{W}_f \rangle_a$ reduces the amplitude of the torsional vibrations; however, if $\beta < 1$, this term amplifies the oscillations until the eventual appearance of a stick–slip limit cycle.

In order to evaluate the influence of the different parameters on the occurrence of the stick–slip vibrations, it is convenient to introduce a measure of how fast the amplitude of the self-excited vibrations grows with time. This measure is taken to be τ_{sk}, which is defined as the time when the bit first sticks. The value of τ_{sk} computed for a set of parameters is not absolute, however, as it depends on the magnitude and the nature of the perturbation. Hence, the curves in Fig. 9, which illustrates the influence on τ_{sk} of the control parameters $\mathscr{W}_o$ and ω_o and of the system parameters β, λ and ψ, have to be interpreted in a relative sense as giving a trend of the balance between self-excitation and damping. Consistent with the explanation that cutting is at the root of the self-excited vibrations and that the frictional contact is damping these vibrations, we can observe from Fig. 9 that τ_{sk} increases with λ but decreases with $\mathscr{W}_o$. Indeed, an increase of the weight-on-bit for a constant state of bluntness of the cutters brings more energy in the pure cutting process, magnifying the self-excited vibrations. The reverse tendency takes place with increasing λ (proportional to the wearflat length) under constant weight-on-bit. An increase of ω_o also tends to mitigate the stick–slip vibrations.

As long as $\beta < 1$, τ_{sk} is increasing with β, as shown in Fig. 9e, this indicates the existence of a vertical asymptote at $\beta = 1$. An augmentation of β for an equivalent level of self-excitation δ causes a rise of the frictional contribution of the torque, which stabilizes the torsional vibrations.

In Fig. 9b the variation of τ_{sk} with ω_o is shown, and these results indicate the existence of two windows for which the bit does not undergo stick–slip vibrations. The left grey window represents the so-called anti-resonance zone, whose existence and characteristics depend on the other parameters of the system. The anti-resonance regime is characterized by a limit cycle described by low amplitudes of vibrations of ω around ω_o as depicted in Fig. 10, even though the transient motion passes through stick–slip phases. A power spectrum analysis reveals also a distinct series of harmonics for each of the variables but the dominant frequency of ω, v and δ does not correspond anymore to the natural torsional frequency of the drill string ($= 1/2\pi$). All these particular cases will be referred to as the anti-resonant response of the system. The second grey window located on the right corresponds to what we describe as a quasi-limit cycle, which is related to an extremely

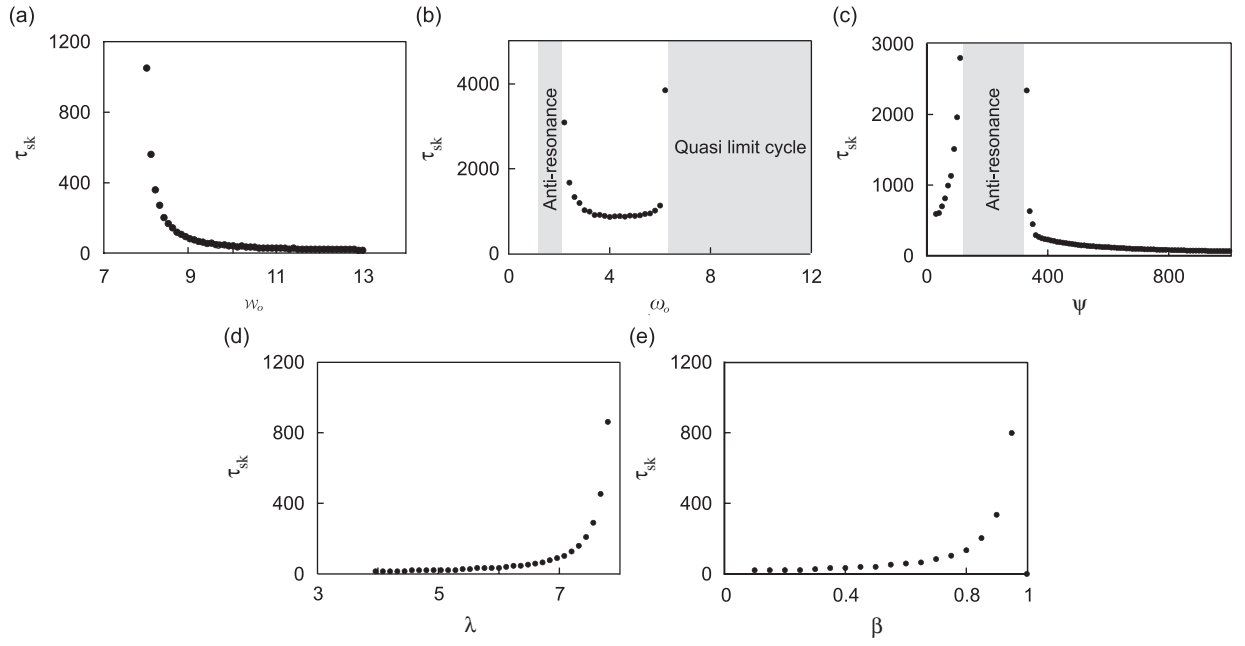

Fig. 9. Variation of τ_{sk} with (a) $\mathscr{W}_o$, (b) ω_o, (c) ψ, (d) λ and (e) β ($n = 6$, $\psi = 63.1$, $\omega_o = 4$, $\mathscr{W}_o = 8$, $\beta = 0.276$, $\lambda = 7.8$ unless parameter is varied).

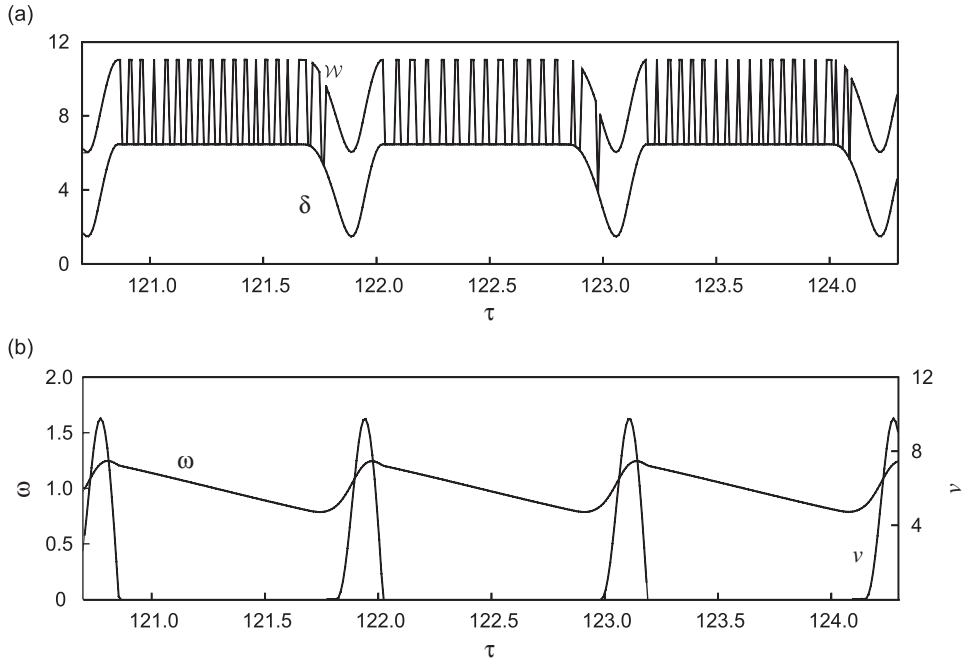

Fig. 10. Evolution with time τ of: (a) δ and $\mathscr{W}$ and (b) ω and v ($n = 6$, $\psi = 63.1$, $\beta = 0.276$, $\omega_o = 1$, $\mathscr{W}_o = 8$, $\lambda = 4.56$).

slow rate of growth of the amplitudes of vibrations. So there is a range of values of ω_o (larger than those corresponding to the anti-resonance regime), for which an increase in the imposed angular velocity leads to a reduction of the occurrences of stick–slip vibrations.

Finally, some range of ψ corresponds to the anti-resonance regime, see Fig. 9c. For values of ψ larger than those associated to the anti-resonance, the reduction of τ_{sk} with ψ indicates that the rate of growth of the torsional vibrations augments with drilling depth due to increasing compliance of the drill pipe system.

5. Mean response of the system

In this section, we focus on the mean response of the system, by averaging over a limit cycle in torsion. A parameter κ ($0 \leqslant \kappa < 1$) is introduced to quantify the intermittent loss of frictional contact caused by axial vibrations. An increase of the angular velocity ω_o and a decrease of the weight-on-bit $\mathscr{W}_o$ is shown to increase on average the relative duration of contact at the wearflat/rock interface, until permanent contact is achieved (corresponding to $\kappa = 0$). In particular, we demonstrate that the average torque-on-bit $\langle \mathscr{T} \rangle$ decreases with increasing ω_o, for $\beta < 1$. This result suggests that the velocity weakening interface law generally assumed to be an intrinsic property of the bit rock interaction is actually a consequence rather than a cause of the self-excited vibrations. We also discuss the conditions leading to bit bouncing.

5.1. Averaging over a limit cycle in torsion

The mean response of the system, $\langle \mathscr{B} \rangle$, can simply be obtained by averaging quantities over a limit cycle in torsion (with the symbol $\langle . \rangle$ used to denote such an average). The non-trivial components of $\langle \mathscr{B} \rangle$ are the mean penetration rate $\langle v \rangle = \langle \dot{u} \rangle + v_o$ (or equivalently $\langle \delta \rangle$ since $\langle v \rangle = \omega_o \langle \delta \rangle / 2\pi$) and the mean torque $\langle \mathscr{T} \rangle$, as $\langle \mathscr{W} \rangle = \mathscr{W}_o$ and $\langle \omega \rangle = \omega_o$ necessarily. Thus, the departure of $\langle v \rangle$ (or $\langle \delta \rangle$) and $\langle \mathscr{T} \rangle$ from the trivial solution v_o (or δ_o) and $\mathscr{T}_o$ is a measure of the effects of vibrations on the bit response. In fact, it can already be concluded from the existence of a limit cycle, together with the discontinuous nature of the contact condition, Eq. (31), that $\langle \delta \rangle \geqslant \delta_o$ and $\langle \mathscr{W}_f \rangle \leqslant \lambda$. The increase of the penetration rate with respect to v_o is thus associated with an intermittent loss of frictional contact caused by axial vibrations. It is convenient to use the parameter κ

defined as

$$\kappa = 1 - \langle \mathscr{W}_f \rangle / \lambda \tag{42}$$

to quantify the level of intermittent loss of frictional contact at the bit–rock interface. In principle, κ can vary between 0 (permanent contact between the chamfers and the rock) to 1 (absence of any frictional contact during drilling). However, as shown below, this upper bound cannot be realistically attained as bit bouncing takes place for $\kappa_k < \kappa < 1$.

The drilling efficiency η is defined as the ratio between the energy devoted to the pure cutting process and the total energy provided to the bit, averaged over a limit cycle; in other words $\eta = \langle \mathscr{T}_c \rangle / \langle \mathscr{T} \rangle$. The efficiency is related to κ according to

$$\eta = \frac{\mathscr{W}_o - \lambda(1-\kappa)}{\mathscr{W}_o - \lambda(1-\kappa)(1-\beta)} \tag{43}$$

and varies therefore between $\eta_o = \delta_o / \mathscr{T}_o$ for $\kappa = 0$ to 1 for $\kappa = 1$.

Considering that the system reaches a periodic motion or a quasi-limit cycle (extremely low evolution of the limit cycle compared to the characteristic time of oscillations), $\langle \ddot{u} \rangle = \langle \ddot{\varphi} \rangle = 0$, we can readily deduce that

$$\mathscr{W}_o = \langle \delta \rangle + (1-\kappa)\lambda, \quad \mathscr{T}_o = \langle \mathscr{T} \rangle + \langle \varphi \rangle. \tag{44}$$

Hence, using Eqs. (21), (30), (25) and (42), we can write $\langle \delta \rangle, \langle \mathscr{T} \rangle$ and $\langle \varphi \rangle$ in terms of κ and the other parameters of the system as

$$\langle \delta \rangle = \delta_o + \kappa\lambda, \quad \langle \mathscr{T} \rangle = \langle \delta \rangle + (1-\kappa)\beta\lambda, \quad \langle \varphi \rangle = -(1-\beta)\kappa\lambda. \tag{45}$$

Deviation of the mean bit response from the trivial solution is thus embodied in the single parameter κ. The meaning of Eq. (45) can be explained as follows. The first equation in Eq. (45) indicates that increased intermittent loss of frictional contact, as measured by κ, yields larger rate of penetration and improved efficiency, as a consequence of an energy transfer ($\kappa\lambda$) from the frictional contact to the pure cutting process. The second equation in Eq. (45) simply expresses that the external power $\langle \mathscr{T} \rangle$ is balanced by the energy devoted to the cutting process, $\langle \delta \rangle$, and the energy dissipated into frictional contact, $(1-\kappa)\beta\lambda$. Finally, the third equation in Eq. (45) shows that the mean elastic energy $\langle \varphi \rangle$ stored in the drill pipes is larger or less than its trivial value ($\langle \varphi \rangle = 0$) depending on whether β is smaller or larger than 1.

5.2. Influence of parameters on κ

Here, we focus on the case $\beta < 1$, which reflects typical bit geometries through γ. An exhaustive analysis of the influence of all the parameters indicate that κ is virtually insensitive to any variations of β and that it depends on $\mathscr{W}_o$ and λ only via the ratio $\mathscr{W}'_o = \mathscr{W}_o / \lambda$, i.e.,

$$\kappa = \kappa(\mathscr{W}'_o, \omega_o, \psi, n). \tag{46}$$

Typical variation of κ with each parameter of the reduced set is depicted in Fig. 11, which shows that κ increases with ψ and $\mathscr{W}'_o$ but decreases with ω_o. These results imply that stronger axial vibrations are associated with increasing depth of drilling, larger weight-on-bit, sharper bit, and reduced rotational speed. The dependence of κ on $\mathscr{W}_o$ and λ only via the ratio $\mathscr{W}_o / \lambda$ reflects that the level of vibrations is controlled by a balance between the energy expended in cutting (self-excitation), and the energy dissipated by frictional contact (damping).

The mean torque $\langle \mathscr{T} \rangle$ can also be expressed in terms of its trivial value $\mathscr{T}_o$ and κ. Combining (44) and (45), we obtain

$$\langle \mathscr{T} \rangle = \mathscr{T}_o + (1-\beta)\kappa\lambda. \tag{47}$$

Referring to the variation of κ with ω_o shown in Fig. 11, we conclude from Eq. (47) that the mean torque $\langle \mathscr{T} \rangle$ decreases with increasing angular velocity ω_o if $\beta < 1$ (the typical case), while it increases with ω_o if $\beta > 1$. In both cases, $\langle \mathscr{T} \rangle$ converges with larger ω_o towards $\mathscr{T}_o$ the torque-on-bit in the absence of any vibrations. These results therefore imply that the velocity weakening interface law generally assumed to be an intrinsic property of the bit rock interaction is actually a consequence rather than a cause of the self-excited vibrations.

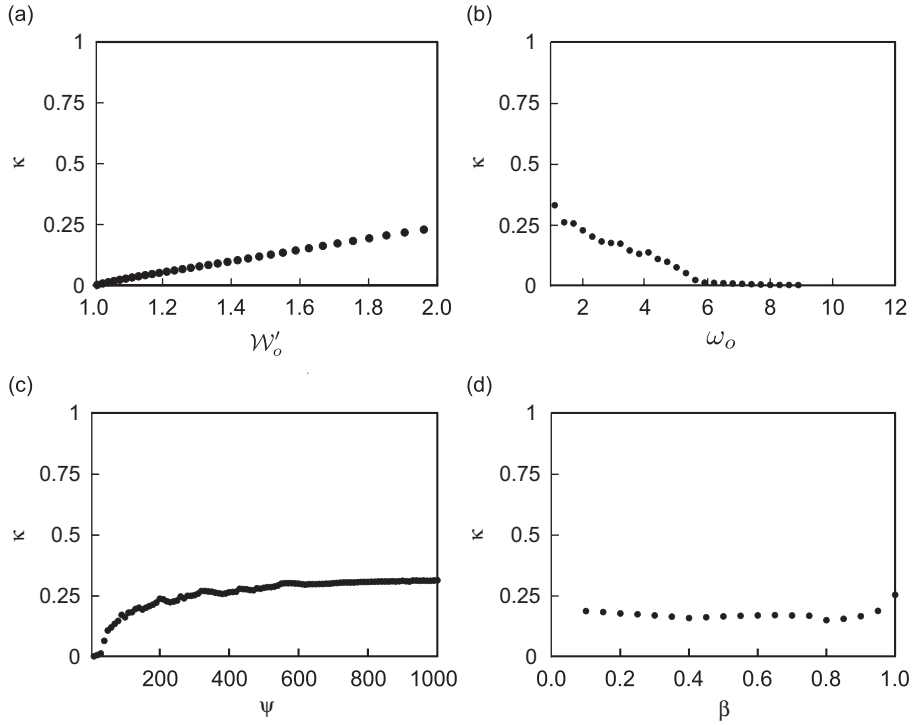

Fig. 11. Variation of κ with (a) $\mathcal{W}'_o$, (b) ω_o, (c) ψ and (d) β ($\mathcal{W}'_o = 1.7$, $\omega_o = 4$, $\psi = 63$, $n = 6$ and $\beta = 0.28$).

The variation of $\langle \mathcal{T} \rangle$ with ω_o is intimately related the intermittent losses of frictional contact occurring at the wearflat/rock interface.

5.3. E-S diagram

A useful tool for assessing the state of the mean bit response is the $\mathcal{E}$-$\mathcal{S}$ diagram [25], where the specific energy $\mathcal{E}$ is plotted versus the drilling strength $\mathcal{S}$. These two quantities are, respectively, defined as

$$\mathcal{E} = \frac{E}{\varepsilon} = \frac{\langle \mathcal{T} \rangle}{\delta}, \quad \mathcal{S} = \frac{S}{\zeta \varepsilon} = \frac{\langle \mathcal{W} \rangle}{\delta}. \tag{48}$$

The rationale for representing the bit response in the $\mathcal{E}$-$\mathcal{S}$ diagram derives from the linear constraint, Eq. (9), between torque-on-bit T, weight-on-bit W, and depth of cut d. In dimensionless form, this relation can be written as

$$\langle \mathcal{T} \rangle = (1 - \beta)\langle \delta \rangle + \beta \langle \mathcal{W} \rangle, \tag{49}$$

which can equivalently be expressed as

$$\mathcal{E} = (1 - \beta) + \beta \mathcal{S} \quad \text{with } \mathcal{E},\ \mathcal{S} \geqslant 1. \tag{50}$$

The above equation identifies the friction line of slope β passing through the cutting point ($\mathcal{E} = \mathcal{S} = 1$). The cutting point corresponds to a maximum efficiency $\eta = 1$, when all the energy provided to the bit is converted into cutting of the rock. Only points on the friction line on the right and above the cutting point are admissible as they correspond to efficiency $\eta = \mathcal{E}^{-1}$ less than unity.

Results of numerical simulations carried out for two particular cases $\beta > 1$ and $\beta < 1$ with several angular velocities are shown on the $\mathcal{E}$-$\mathcal{S}$ diagram in Fig. 12. The point representative of the bit response moves

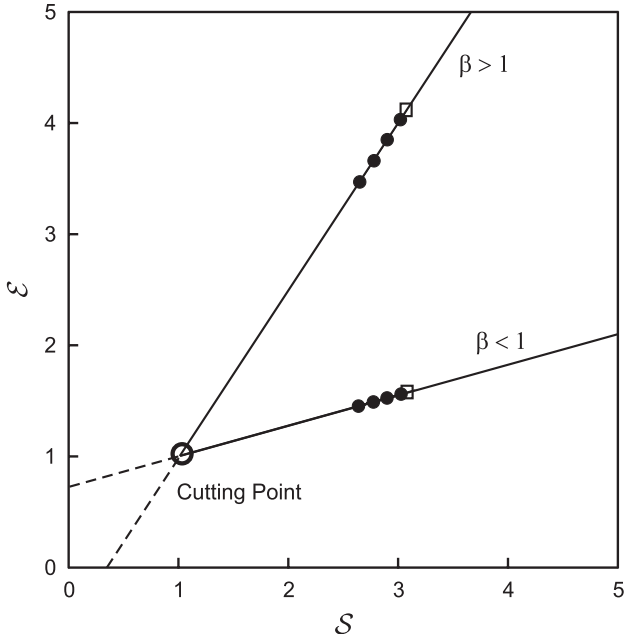

Fig. 12. $\mathscr{E}-\mathscr{S}$ diagram for $\beta=0.276$ and $\beta=1.5$ ($\mathscr{W}_o=8,\ \psi=100,\ \lambda=0.9,\ n=6$). The white squares correspond to the trivial solutions.

upwards along the friction line with increasing angular velocity, meaning that η decreases with ω_o. Furthermore, the points converge towards the point representative of the trivial solution, i.e., the state of minimum efficiency η_o, which occurs in the absence of vibrations.

5.4. Bit bouncing and drilling efficiency

From numerical experiments there is evidence of the existence of an upper bound $\mathscr{W}'_{ok}(\omega_o,\psi,n)$ for $\mathscr{W}'_o$ beyond which the axial vibrations are so important that it causes the bit to bounce. Because κ increase with $\mathscr{W}'_o$, these results imply not only the existence of an upper bound $\kappa_k(\omega_o,\psi,n)$ below which bit bouncing is prevented, but also an upper bound $\langle\delta\rangle_k=\mathscr{W}_o-\lambda\kappa_k(\omega_o,\psi,n)$ to the depth of cut (or equivalently to the rate of penetration). With increasing axial vibrations, $\langle\delta\rangle$ can therefore increases from the trivial value $\delta_o=\mathscr{W}_o-\lambda$ to a maximum $\langle\delta\rangle_k$, which is however always less than the depth of cut per revolution $\delta_{\max}=\mathscr{W}_o$ that can be achieved with an ideally sharp bit. Fig. 13 illustrates these results for different ω_o and ψ. Both control parameters $(\omega_o,\mathscr{W}_o)$ and their influences are presented here. Moreover, via the ratio $\mathscr{W}'_o$, sharp bit or large weight-on-bit increase the susceptibility to bit bouncing. By increasing ω_o, drilling becomes more stable whatever the set $(\mathscr{W}_o,\lambda)$ chosen. However, this increase of stability is accompanied with a decrease of the drilling efficiency since the points migrate towards the trivial rate of penetration ($\kappa\simeq 0$). As depicted in Fig. 13, the risk of bit bouncing increases with ψ, for example when drilling deeper as the system of pipes becomes more compliant. On the one hand, reducing ψ stabilizes the bit motion, but on the other hand it decreases the drilling efficiency. Fig. 14 (a) displays the enlargement of the region of bit bouncing with the parameter ψ in the space of control parameters $(\mathscr{W}_o,\omega_o)$, while Fig. 14 (b) shows the corresponding variation of the drilling efficiency η for $\psi=100$.

6. Conclusions

In this paper, we have proposed a novel model to investigate the self-excited vibrations of a drilling system. This model differs from other published approaches in two significant ways. First, we have considered both the axial and torsional vibrations of the bit, as well as the coupling between the two vibration modes through

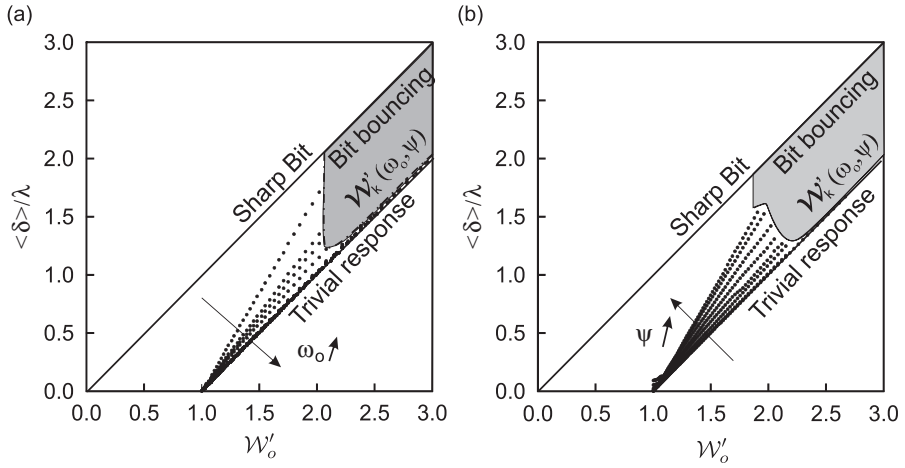

Fig. 13. Variation of $\langle\delta'\rangle$ with $\mathcal{W}'_o$ for different values of (a) ω_o $(1, 3, 4, 7, 8.2, 8.4)$, and (b) ψ $(20, 30, 40, 60, 100, 200, 500, 1000)$, with $n = 6$, $\psi = 63.1, \omega_o = 4$, $\beta = 0.276$.

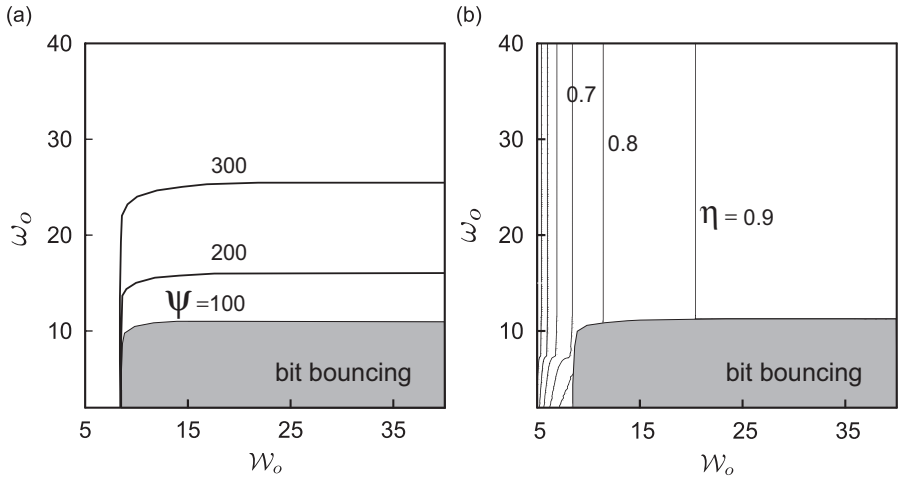

Fig. 14. (a) Variation of region of bit bouncing with ψ, and (b) variation of drilling efficiency η (for $\psi = 100$) in the space of control parameters ($\mathcal{W}_o$, ω_o) when $n = 6$, $\lambda = 4.2$ and $\beta = 0.43$.

bit–rock interaction laws that account for both cutting and frictional contact. Second, we have included rate-independent bit–rock interaction laws, which are consistent with laboratory results from single cutter experiments.

The critical elements that have been incorporated in this model are: (i) the axial inertia of the bottom hole assembly; (ii) the particular nature of the boundary conditions at the bit–rock interface that are associated with the cutting process; and (iii) the potential loss of contact across the chamfer or wearflat. All parameters introduced in the model are measurable quantities. The resulting model is an unusual state-dependent delay dynamical system, with discontinuous boundary conditions.

A linear stability analysis confirms that the trivial motion of the bit is unstable and numerical simulations show that any perturbation triggers self-excited vibrations of the system. The delayed and coupled nature of the cutting process is responsible for the self-excited nature of the induced vibrations. Moreover, the loss of contact that accompanies any upward motion of the bit routes most of the energy from the axial into the torsional mode of vibrations and is essential to avoid bit bouncing ($d < 0$).

The features of the induced torsional and axial oscillations are coherent with field measurements and observations. A parametric analysis in fact indicates that, in the space of dimensionless parameters, the region associated to a high susceptibility to stick–slip corresponds well to typical field quantities.

The number $\beta = \mu\gamma\zeta$ appears as a dominant parameter of the problem. It strongly affects the propensity of the system to stick–slip. According to numerical results, the condition $\beta \geqslant 1$ appears to be sufficient to preclude the appearance of stick–slip vibrations at least in a range of parameters that are typical of field cases. On the other hand, $\beta < 1$ is a necessary but not sufficient condition for instability to arise and stick–slip to occur.

Finally, results of numerical simulations indicate that apparent rate effects are inherent to the model. An increase of the imposed angular velocity ω_o results in a decrease of the average depth of cut. The state of minimum efficiency (corresponding to the trivial depth of cut) occurs in the absence of vibrations, which is reached asymptotically when ω_o is large, i.e., when the period of the resonant torsional vibration becomes large compared to the time taken by one revolution of the bit. Since the average weight-on-bit is necessarily equal to $\mathscr{W}_o$, the variation of the average torque $\langle T \rangle$ with ω_o is controlled by the magnitude of β; namely, $\langle T \rangle$ decreases with ω_o if $\beta < 1$, but increases with ω_o if $\beta > 1$. In fact, one of the most important results of this research is that the apparent rate effect is an outcome rather than an input to the model.

One of the main limitations of this model is the reduction of the drillstring to a two degrees of freedom system. Work is currently underway to model the drillstring using the finite element method, so as to capture more modes of vibrations [50]. Preliminary numerical simulations show that there are many cases where the results obtained with the finite element model are consistent with those predicted by the low-order model, but there are also a few situations where stick–slip occurs at frequencies higher than the first torsional mode.

Acknowledgments

The research was supported by grants from BP-Amoco (UK), Security-DBS (USA), Diamant Drilling Services (Belgium), and CSIRO (Australia) and by a Sommerfeld fellowship from the Department of Civil Engineering of the University of Minnesota. The authors are in particular indebted to Martyn Fear from BP-Amoco for bringing them the reality of field data and for his confidence in the research team. The authors would also like to recognize the contributions of Dr. T. Insperger (Budapest University of Technology and Economics) and Prof. R. Sepulchre (University of Liège) in the formulation of the linear stability analysis. Finally the authors would like to thank one of the reviewers for his careful critique of the original manuscript and for valuable comments which have enabled us to improve the paper.

Appendix A

In this appendix, we present an analysis of the results of a series of full-scale laboratory drilling experiments, carried out in a Mancos shale with a step-type 8.5 in diameter PDC bit for various combinations of imposed Ω_o and W_o ($W_o = 40, 80, 120$ kN and Ω_o varying between 50 and 900 rev/min) [11]. These data are of particular interest because they provide experimental evidence of the bit–rock interaction laws summarized in Section 2.2, but also because they clearly display a decrease of the mean torque with the imposed angular velocity.

The bit–rock interaction is characterized by a linear constraint between the specific energy $E = 2T/a^2 d$ and the drilling strength $S = W/ad$ [25]:

$$E = E_o + \mu\gamma S, \tag{A.1}$$

where $E_o = (1 - \beta)\varepsilon$. In fact, Eq. (A.1) is the dimensional equivalent of Eq. (50). In the E-S diagram (see Fig. A.1(a)), the point representative of the bit response lies on the friction line. Its location along the line is related to the drilling efficiency $\eta = \varepsilon/E$, or equivalently to the fraction of the weight-on-bit transmitted by the contact area between the bit and the rock. If the bit is sharp, the state point is located at the cutting point ($E = \varepsilon$, $S = \zeta\varepsilon$), otherwise the point migrates upwards along the friction line with decreasing efficiency. It can also readily be established that a decrease of efficiency is accompanied by a decrease of the average torque under constant weight-on-bit if $\beta < 1$ (and by an increase of torque if $\beta > 1$).

The overall response of the laboratory tests is summarized in the E-S diagram shown in Fig. A.1(b). Clearly, all the experimental data lay along the same line regardless of the angular velocity. Therefore, neither the intrinsic specific energy ε nor the apparent friction coefficient $\mu\gamma$ between the bit and the rock varies with the angular velocity ($\varepsilon \simeq 230$ MPa, $\mu\gamma \simeq 0.48$). However, the dispersion along the friction line is large; the points representative of the bit response move upwards along the friction line with increasing angular velocity, under constant weight-on-bit. Furthermore, as can be seen in Fig. A.2, the mean torque decreases with increasing Ω_o under constant W_o, consistent with a value of $\beta < 1$ ($\beta \simeq 0.35$).

The diminishing efficiency η with larger Ω_o under constant W_o reflects an increase of the contact forces at the expense of the forces mobilized by the cutting process. In principle, a reduction of η could be associated with either an increase of the overall contact area or with an increase of the mean contact stress acting across the wearflats with Ω_o. However, change of the contact area between the bit and the rock due either to bit wear and/or inadequate bottom-hole cleaning with increasing Ω_o is unlikely under these laboratory conditions. Indeed, the short drilled length and the non-abrasive nature of the Mancos shale rule out a possible wear of the bit over the duration of these tests. Also, cleaning problems would result in an evolving contact distribution between the bit and the hole-bottom. However, the corresponding change in the bit geometry number γ (as reflected by the slope of the friction line) is not observed in the data set. More importantly, any

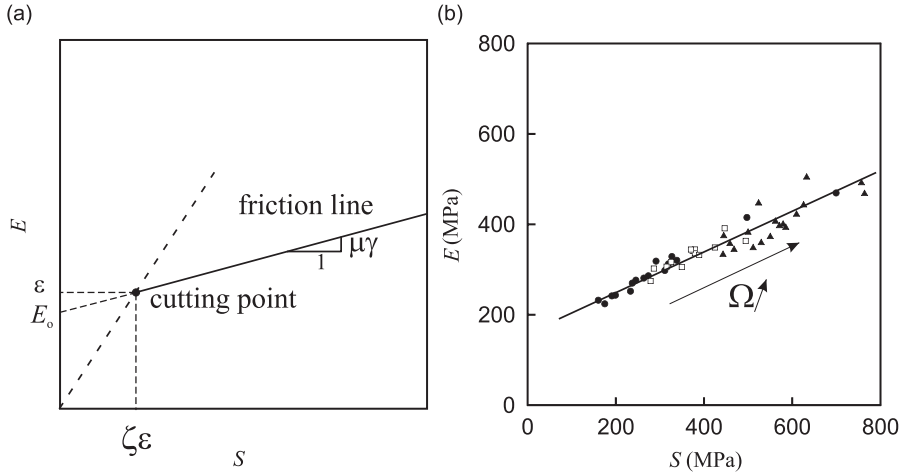

Fig. A.1. (a) Conceptual sketch of the E-S diagram, and (b) E-S diagram, according to published experimental data [11] with ▲$W = 40$ kN, □ $W = 80$ kN, • $W = 120$ kN.

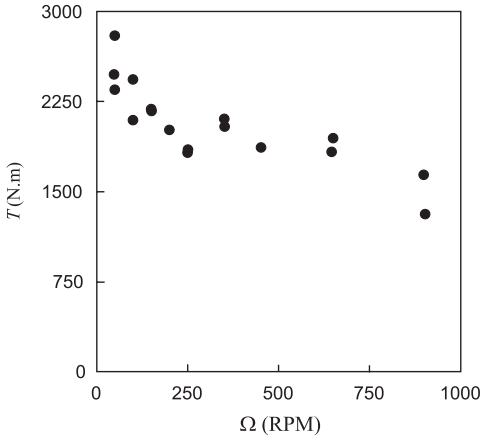

Fig. A.2. Evolution of the mean torque $\langle T \rangle$ with the angular velocity Ω_o under constant weight-on-bit ($W = 120$ kN), according to published experimental data [11].

variation of the torque due to inadequate removal of debris flow would happen over a time scale equivalent to several rotations, too large to be compatible with the time scale of the stick–slip oscillations.

The only remaining explanation is an increase of the mean contact stress σ with Ω_o. Assuming permanent contact between the bit flat and the rock, σ would have to increase with the relative velocity between the wearflat and the rock. Although such a law cannot be ruled out a priori, no significant effect of the cutting velocity on the forces has been reported in the literature. However, the mean contact stress could increase with Ω_o if axial vibrations responsible for an intermittent loss of contact between the bit and the rock progressively decrease in intensity with Ω_o. Such a result is actually predicted by the model discussed in the body of this paper.

Interpretation of the laboratory drilling data [11] within the framework of the bit–rock interaction laws can be summarized as follows: (i) the bit response is consistent with a bit–rock interaction model which takes into account both the cutting and frictional processes mobilized at the bit–rock interface [25]; (ii) the rate effects are real but they are not a constitutive property of the bit–rock interface, in the sense that they do not affect the parameters of the model (ε, ζ, μ, γ); (iii) the rate effects are associated with an increase of the mean contact stress transmitted at the flat–rock interface with Ω_o.

Appendix B

In this appendix, we investigate the stability of the equilibrium point $u = \text{Constant}$ (equivalent to $u = \breve{u}$) of the delay differential equation:

$$\ddot{u} + n\psi u - n\psi \breve{u} = 0 \tag{B.1}$$

governing the axial perturbation u. Consider the characteristic equation of Eq. (B.1)

$$P(s) = s^2 + n\psi(1 - \mathrm{e}^{-s\tau_n}). \tag{B.2}$$

The location of the roots of $P(s)$ in the complex plane will determine the stability of $\dot{u} = 0$. Because one root is always located at the origin, we study instead the modified characteristic function

$$Q(s) := \frac{P(s)}{s} = s + \frac{n\psi}{s}(1 - \mathrm{e}^{-s\tau_n}). \tag{B.3}$$

The equilibrium point $\dot{u} = 0$ is asymptotically stable if and only if all the roots satisfying $Q(s) = 0$ are located on the left of the imaginary axis of the complex plane s. When $\tau_{no} = 0$, one root is located at the origin, and the solution $\dot{u} = 0$ is thus stable in the Lyapunov sense.

When the equation becomes retarded ($\tau_{no} > 0$), there exists an infinite number of roots. From Eq. (B.3) and because $|(1 - \mathrm{e}^{-s\tau_n})| < 2$ when $\mathrm{Re}\{s\} > 0$ and $\tau_{no} > 0$, any roots with positive real part must lie within the half-circle centered on the origin of radius $\sqrt{2n\psi}$ ($|s| < \sqrt{2n\psi}$). Let us choose τ_{no} sufficiently small such that $1 - \mathrm{e}^{-s\tau_{no}} \approx s\tau_{no}$ for any s satisfying $|s| < \sqrt{2n\psi}$. The only root inside this circle is

$$s_o = -n\psi\tau_{no}. \tag{B.4}$$

Therefore, the root located at the origin for zero delay moves left for small τ_{no}. We can conclude that there is no root with positive real part for $\tau_{no} \ll 1$ and that the equilibrium point $\dot{u} = 0$ is asymptotically stable.

Next, let us study the root locus $s(\tau_{no})$ given by the implicit equation

$$s^2 + n\psi(1 - \mathrm{e}^{-s\tau_{no}}) = 0. \tag{B.5}$$

Although the solution $\dot{u} = 0$ is asymptotically stable for small value of the delay, a bifurcation will occur if one root traverses the imaginary axis from left to right for larger τ_{no}. Let us compute the values of $s = \mathrm{i}\bar{\omega}_k, \tau_{no,k}$ such that

$$-\bar{\omega}_k^2 + n\psi(1 - \mathrm{e}^{-\mathrm{i}\bar{\omega}_k\tau_{no,k}}) = 0. \tag{B.6}$$

The non-trivial solutions of Eq. (B.6) are given by

$$\bar{\omega}_k = \pm\sqrt{2n\psi} \quad \text{when } \tau_{no,k} = \frac{(2k+1)\pi}{\sqrt{2n\psi}}. \tag{B.7}$$

Moreover, the direction of travel of the roots with τ_{no} can be deduced from the derivative $ds/d\tau_{no}$ on the root locus $P(s)=0$, which can be deduced from

$$\frac{dP(s)}{d\tau_{no}} = \frac{\partial P}{\partial s}\frac{ds}{d\tau_{no}} + \frac{\partial P}{\partial \tau_{no}} = 0 \tag{B.8}$$

and therefore,

$$\left.\frac{ds}{d\tau_{no}}\right|_{P=0} = -\frac{n\psi s e^{-s\tau_n}}{2s + n\psi\tau_n e^{-s\tau_n}}. \tag{B.9}$$

By looking at the real part of Eq. (B.9) at the crossing points $s=\pm i\sqrt{2n\psi}$, for $\tau_{no}=(2k+1)\pi/\sqrt{2n\psi}$, we obtain a strictly positive quantity

$$\mathrm{Re}\left\{\left.\frac{ds}{d\tau_{no}}\right|_{P(s)=0}\right\} = \frac{8n\psi}{16+(2k+1)^2\pi^2} > 0. \tag{B.10}$$

The two complex conjugate roots will pass from the left half-plane to the right half-plane at the first crossing $\tau_{no,o}=\pi/\sqrt{2n\psi}$ and will remain in the right half-plane. We can thus conclude that when $\tau_{no}<\pi/\sqrt{2n\psi}$, the equilibrium point $\dot{u}=0$ and $u(\tau)-u(\tau-\tau_{no})=0$ is asymptotically stable, marginally stable when $\tau_{no}=\pi/\sqrt{2n\psi}$ and unstable when $\tau_{no}>\pi/\sqrt{2n\psi}$.

Appendix C

In this appendix the numerical procedure used to solve the nonlinear system described by Eqs. (25)–(33) is given. First, the two second-order differential equations (Eq. (25)) are reduced to four first-order differential equations that are solved by using a simple Euler-forward finite difference technique. Although other algorithms have been implemented (such as second and fourth-order Runge–Kutta method), the Euler algorithm was preferred because it is numerically more efficient at comparable level of accuracy for this class of problems.

A critical element of the procedure is the calculation of the delay perturbation $\hat{\tau}_n(\tau)$. In order to solve Eq. (28) for $\hat{\tau}_n(\tau)$, it is necessary to keep the time history of the bit angular position over the last angular section of angle $2\pi/n$ covered by the bit prior to time τ. Also the time history of the bit axial position has to be saved to compute the depth of cut at time τ. Finally, the bit axial velocity at the previous time step $\tau-\Delta\tau$ ($\Delta\tau$ being the time increment) is needed to assess the possible loss of contact at time τ.

The solution is advanced from time τ to the next time step $\tau+\Delta\tau$ as follows:

1. The new values of u, $\dot{u}$, φ, $\dot{\varphi}$ at time $\tau+\Delta\tau$ are computed from

$$\begin{aligned}
\dot{u}(\tau+\Delta\tau) &= \dot{u}(\tau) + \psi[\mathscr{W}_o - \mathscr{W}(\tau)]\Delta\tau,\\
u(\tau+\Delta\tau) &= u(\tau) + \dot{u}(\tau+\Delta\tau)\Delta\tau,\\
\dot{\varphi}(\tau+\Delta\tau) &= \dot{\varphi}(\tau) + [\mathscr{T}_o - \mathscr{T}(\tau)]\Delta\tau - \varphi(\tau)\Delta\tau,\\
\varphi(\tau+\Delta\tau) &= \varphi(\tau) + \dot{\varphi}(\tau+\Delta\tau)\Delta\tau.
\end{aligned} \tag{C.1}$$

2. The delay perturbation $\hat{\tau}_n(\tau)$ is determined from Eq. (28) by interpolating between two discrete values of the angular motion history.
3. The depth of cut is then computed from Eqs. (26) and (27); $\tilde{u}(\tau)=u(\tau-\tau_n)$ is interpolated between two discrete values of the axial motion history. If bit bouncing occurs (i.e. $\delta<0$) the program is interrupted.
4. The forces ($\mathscr{T}$, $\mathscr{W}$) are updated according to Eqs. (29)–(31); in particular, $\mathscr{W}_f$ is set to zero if loss of contact occurs, i.e., $\dot{u}(\tau)<0$.
5. The stick condition given in Eq. (32) is checked. If it is fulfilled, the angular position when the bit exits the stick phase and starts to slip is computed using Eq. (33) and the time is updated by the duration of the stick phase.

The explicit nature of the finite difference code does not guarantee stability. Numerical simulations indicate that the rapid variation of the depth of cut imposes a relatively small time step ($\Delta\tau \sim 10^{-5}$–10^{-4}) to avoid the occurrence of numerical instability.

References

[1] B. Feeny, A. Guran, N. Hinrichs, K.A. Popp, Historical review on dry friction and stick–slip phenomena, *Applied Mechanics Reviews* 51 (5) (1998) 321–341.

[2] R.A. Ibrahim, Friction-induced vibration, chatter, squeal, and chaos. Part I: mechanics of contact and friction, *Applied Mechanics Reviews* 47 (7) (1994) 209–226.

[3] J. Dieterich, Modeling of rock friction 1. Experimental results and constitutive equations, *Journal of Geophysical Research* 84 (15) (1979) 2161–2168.

[4] J. Dieterich, Modeling of rock friction 2. Simulation of preseismic slip, *Journal of Geophysical Research* 84 (15) (1979) 2169–2175.

[5] J. Rice, A. Ruina, Stability of steady frictional sliding, *Journal of Applied Mechanics* 50 (2) (1983) 343–349.

[6] V. Oancea, T. Laursen, Stability analysis of state dependent dynamic frictional sliding, *International Journal of Non-Linear Mechanics* 32 (5) (1997) 837–853.

[7] S.W. Shaw, On the dynamic response of a system with dry friction, *Journal of Sound and Vibrations* 108 (2) (1986) 305–325.

[8] V. Migouline, V. Medvedev, *Fondements de la Théorie des Oscillations*, Mir Moscow, 1988.

[9] K. Popp, N. Hinrichs, M. Oestreich, Analysis of a self-excited friction oscillator with external excitation, *Dynamics with Friction: Modeling, Analysis and Experiment*, Series on Stability Vibrations and Control of Systems Series B, Vol. 7, World Scientific Publishing Company, Singapore, 1996, pp. 1–35.

[10] A.A. Andronov, A.A. Vitt, S.E. Khaikin, *Theory of Oscillators*, Dover, 1966.

[11] A.D. Black, B.H. Walker, G.A. Tibbitts, J.L. Sandstrom, PDC bit performance for rotary, mud motor, and turbine drilling applications, *SPE Drilling Engineering* 1 (6) (1986) 409–416 (Paper No. 13258-PA).

[12] M.J. Fear, F. Abbassian, S.H.L. Parfitt, A. McClean, The destruction of PDC bits by severe stick–slip vibrations, *presented at SPE/1ADC Drilling Conference*, Society of Petroleum Engineers Paper No. 37369-MS, Amsterdam, Netherlands, 4–6 March 1997, pp. 1–11.

[13] J.F. Brett, The genesis of torsional drillstring vibrations, *SPE Drilling Engineering* 7 (Sept.) (1992) 168–174 Paper No. 21943-PA.

[14] V.A. Palmov, E. Brommundt, A.K. Belyaev, Stability analysis of drillstring rotation, *Dynamics and Stability of Systems* 10 (2) (1995) 99–110.

[15] N. Challamel, Rock destruction effect on the stability of a drilling structure, *Journal of Sound and Vibration* 233 (2) (2000) 235–254.

[16] R.W. Tucker, C. Wang, An integrated model for drill-string dynamics, *Journal of Sound and Vibration* 224 (1) (1999) 123–165.

[17] J.A.C. Martins, J.T. Oden, F.M.F. Simões, A study of static and kinetic friction, *International Journal of Engineering Science* 28 (1) (1990) 29–92.

[18] W.W. Twozydlo, E.B. Becker, J.T. Oden, Numerical modeling of friction-induced vibrations and dynamic instabilities, *Applied Mechanics Reviews* 47 (7) (1994) 255–274.

[19] T. Richard, E. Detournay, Stick-slip motion in a friction oscillator with normal and tangential mode coupling, *Compte Rendus de l'Académie des Sciences 328 Series II b* (2000) 1–8 (Transactions of the [French] Academy of Sciences).

[20] D.M. Tolstoi, Significance of the normal degree of freedom and natural normal vibrations in contact friction, *Wear* 10 (1967) 199–713.

[21] G. Adams, Self-excited oscillations of two elastic half-spaces sliding with a constant coefficient of friction, *Journal of Applied Mechanics* 62 (2) (1995) 867–972.

[22] G. Adams, Steady sliding of two elastic half-spaces with friction reduction due to interface stick–slip, *Journal of Applied Mechanics* 65 (2) (1998) 470–475.

[23] F. Simões, J.A.C. Martins, Instability of ill-posedness in some friction problems, *International Journal of Engineering Science* 36 (1998) 1265–1293.

[24] F. Moirot, Q. Nguyen, An example of stick–slip waves, *Compte Rendus de l'Académie des Sciences* (Transactions of the [French] Academy of Sciences) 328 (Série IIb) (2000) 663–669.

[25] E. Detournay, P. Defourny, A phenomenological model of the drilling action of drag bits, *International Journal of Rock Mechanics and Mining Sciences* 29 (1) (1992) 13–23.

[26] J. Tlusty, M. Polacek, The stability of machine tool against self-excited-vibrations in machining, *Proceedings of the American Society of Mechanical Engineering Production Engineering Research Conference*, 1963.

[27] G. Stépàn, Delay-differential equation models for machine tool chatter, in: F.C. Moon (Ed.), *Dynamics and Chaos in Manufacturing Processes*, Wiley, New York, 1998, pp. 165–191.

[28] R.P.H. Faassen, N.V. de Wouw, J.A.J. Oosterling, H. Nijmeijer, Prediction of regenerative chatter by modeling and analysis of high-speed milling, *International Journal of Machine Tool and Manufacture* 43 (2003) 1437–1445.

[29] T. Insperger, G. Stepan, J. Turi, State-dependent delay model for regenerative cutting processes, *Proceedings of ENOC 2005*, Eindhoven, 2005, pp. 1124–1129.

[30] D.W. Dareing, J.L. Tlusty, C.A. Zamudio, Self-excited vibrations induced by drag bits, *Journal of Energy Resources Technology* 112 (1990) 54–61.

[31] C.J. Langeveld, PDC bit dynamics, *presented at the SPE/1ADC Drilling Conference*, Society of Petroleum Engineers Paper No. 23867-MS, New Orleans, Louisiana, 18–21 February 1992, p. 227.
[32] M.A. Elsayed, R.L. Wells, D.W. Dareing, K. Nagirimadugu, Effect of process damping on longitudinal vibrations in drillstrings, *Journal of Energy Resources Technology* 116 (1994) 129–135.
[33] M.A. Elsayed, D.W. Dareing, C.A. Dupuy, Effect of downhole assembly and polycrystalline diamond compact (PDC) bit geometry on stability of drillstrings, *Journal of Energy Resources Technology* 119 (3) (1997) 159–163.
[34] M.A. Elsayed, D.W. Dareing, M.A. Vonderheide, Effect of torsion on stability, dynamic forces, and vibration characteristics in drillstrings, *Journal of Energy Resources Technology* 119 (3) (1997) 11–19.
[35] A. Baumgart, Stick-slip and bit-bounce of deep-hole drillstrings, *Journal of Energy Resources Technology* 122 (2000) 78–82.
[36] J. Den Hartog, *Mechanical Vibrations*, McGraw-Hill, New York, 1956.
[37] F. Abbassian, V.A. Dunayevsky, Application of stability approach to bit dynamics, *Society of Petroleum Engineers Drilling & Completion* 13 (2) (1998) 99–107 (Paper No. 30478-PA).
[38] T. Richard, E. Detournay, A. Drescher, P. Nicodème, D. Fourmaintraux, The scratch test as a means to measure strength of sedimentary rocks, *presented at SPE/ISRM Rock Mechanics in Petroleum Engineering*, Society of Petroleum Engineers Paper No. 47196-MS, Trondheim, Norway, 8–10 July 1998.
[39] E. Detournay, C. Atkinson, Influence of pore pressure on the drilling response in low-permeability shear-dilatant rocks, *International Journal of Rock Mechanics and Mining Sciences* 37 (7) (2000) 1091–1101.
[40] R. Almenara, E. Detournay, Cutting experiments in sandstones with blunt PDC cutters, *Proceedings of EuRock '92*, Thomas Telford, London, 1992, pp. 215–220.
[41] J.I. Adachi, E. Detournay, A. Drescher, Determination of rock strength parameters from cutting tests, *Proceedings 2nd North American Rock Mechanics Symposium (NARMS 1996)*, Balkema, Rotterdam, 1996, pp. 1517–1523.
[42] T. Lhomme, Frictional contact at a Rock–tool Interface: An Experimental Study Masters Thesis, University of Minnesota, 1999.
[43] G. Stépàn, *Retarded Dynamical System*, Longman, London, 1989.
[44] F. Hartung, Linearized stability in periodic functional differential equations with state-dependent delays, *Journal of Computational and Applied Mathematics* 174 (2) (2005) 201–211.
[45] H.K. Khalil, *Nonlinear Systems*, second ed., Prentice-Hall, Englewood Cliffs, NJ, 1996.
[46] S.J. Bhatt, C.S. Hsu, Stability criteria for second-order dynamical systems with time lag, *Journal of Applied Mechanics* 33 (1) (1966) 113–118.
[47] C.S. Hsu, S.J. Bhatt, Stability charts for second-order dynamical systems with time lag, *Journal of Applied Mechanics* 33 (1) (1966) 119–124.
[48] C. Germay, N.V. de Wouw, R. Sepulchre, H. Nijmeijer, Axial stick–slip limit cycling in drill-string dynamics with delay, *Proceedings of ENOC-2005*, Eindhoven, Netherlands, August 2005.
[49] C. Germay, Stability Analysis of PDC Bits, PhD Thesis, University of Liège, Belgium, 2007.
[50] C. Germay, V. Denoel, E. Detournay, Self-excited vibrations of a drilling system with drag bits, *Compte Rendus de l'Académie des Sciences* (Transactions of the [French] Academy of Sciences), to be submitted.